Catena 110 (2013) 32–43

Contents lists available at SciVerse ScienceDirect

Catena

journal homepage: www.elsevier.com/locate/catena

Characterisation of flash floods in small ungauged mountain basins of Central Spain using an integrated approach

V. Ruiz-Villanueva [a,c,*], A. Díez-Herrero [a,1], J.M. Bodoque [b], J.A. Ballesteros Cánovas [a,c], M. Stoffel [c,d]

[a] Department of Research and Geoscientific Prospective, Geological Survey of Spain (IGME), Ríos Rosas 23, Madrid E-28003, Spain
[b] Mining and Geological Engineering Department, University of Castilla La Mancha, Campus Fábrica de Armas, Avda. Carlos III, Toledo E-5071, Spain
[c] Laboratory of Dendrogeomorphology, Institute of Geological Sciences, University of Berne, 3012 Berne, Switzerland
[d] Climatic Change and Climate Impacts, Institute for Environmental Sciences, University of Geneva, 1227 Carouge, Switzerland

ARTICLE INFO

Article history:
Received 28 August 2012
Received in revised form 30 May 2013
Accepted 16 June 2013

Keywords:
Historical floods
Palaeohydrology
Dendrogeomorphology
Ungauged basins
Flood frequency analysis

ABSTRACT

One of the main problems of flood hazard assessment in ungauged or poorly gauged basins is the lack of runoff data. In an attempt to overcome this problem we have combined archival records, dendrogeomorphic time series and instrumental data (daily rainfall and discharge) from four ungauged and poorly gauged mountain basins in Central Spain with the aim of reconstructing and compiling information on 41 flash flood events since the end of the 19th century. Estimation of historical discharge and the incorporation of uncertainty for the at-site and regional flood frequency analysis were performed with an empirical rainfall–runoff assessment as well as stochastic and Bayesian Markov Chain Monte Carlo (MCMC) approaches. Results for each of the ungauged basins include flood frequency, severity, seasonality and triggers (synoptic meteorological situations). The reconstructed data series clearly demonstrates how uncertainty can be reduced by including historical information, but also points to the considerable influence of different approaches on quantile estimation. This uncertainty should be taken into account when these data are used for flood risk management.

1. Introduction

The evaluation of floods occurring in small mountain basins requires an accurate definition of the spatial and temporal distribution of rainfall and discharge, for which an extensive network of precipitation and streamflow gauging stations is needed. However, this type of network is rarely available in mountain areas in general and in Spain in particular (Rico et al., 2001). Hence, much of the instrumental data available is from too short a period to yield reliable and representative information, thus adding considerable uncertainty to the determination of large return periods of catastrophic events (Brázdil et al., 2006). In more general terms, the consequent lack of data largely hampers the analysis of flood magnitude and frequency and calls for the application of alternative or complementary approaches.

Documentary records (such as systematic records by the government, ecclesiastical archives or newspaper reports) have been considered as an alternative source of data with respect to historical floods (Barriendos and Coeur, 2004; Benito et al., 2004). Eyewitness reports on floods in ungauged basins have also been used in the past and constitute yet another source of information in historical hydrology and palaeohydrology (Benito et al., 2003a, 2003b; Brázdil et al., 2006; Thorndycraft et al., 2006). The transformation of these qualitative data into numerical values is standard practise in studies on historical climatology or palaeohydrology (Barriendos and Coeur, 2004; Brázdil et al., 2005, 2010; Martín-Vide and Barriendos, 1995).

The most accurate source of palaeofloods is the identification of palaeostage evidence, such as flood sediments, erosional landforms, driftwood or damage to vegetation (Benito and Thorndycraft, 2005). As mountain rivers are normally characterised by high stream power and high sediment transport rates (Johnson and Warburton, 2002), resulting in a highly variable and changing morphology, flood sediments may not necessarily be either deposited or preserved. At the same time, however, mountain basins are often forested and the coarse-grained sediment and/or woody debris transported by floods may cause damages to trees. This damage will typically cause specific growth reactions in trees (i.e., dendrogeomorphology; Alestalo, 1971; Stoffel and Wilford, 2012), thus enabling past (flash) floods to be dated (Yanosky and Jarrett, 2002). The potential of dendrogeomorphic reconstructions of past events in ungauged basins

* Corresponding author at: University of Bern, Institute of Geological, Sciences Exogene Geology Baltzerstrasse 1+3 CH-3012. Tel.: +41 31 631 87 72.
E-mail address: virginia.ruiz@dendrolab.ch (V. Ruiz-Villanueva).
[1] Associated researcher to IMDEA Agua.

0341-8162/$ – see front matter © 2013 Elsevier B.V. All rights reserved.
http://dx.doi.org/10.1016/j.catena.2013.06.015

and the value of this data for flash flood research have been demonstrated in various studies over the past few years (Ballesteros et al., 2010a, 2010b; Ballesteros Cánovas et al., 2011a, 2011b; Díez-Herrero et al., in press; Ruiz-Villanueva et al., 2010). In addition to yielding information on the frequency or spatial extent of past events, information conserved in tree-ring records also enables the reconstruction of events with at least annual and sometimes even seasonal precision (Stoffel and Bollschweiler, 2008), and may, moreover, provide information regarding river dynamics (Arbellay et al., 2012).

Based on the above considerations, this study takes into account non-instrumental data sources (tree-ring records and documents) in order to improve at-site and regional FFA in ungauged and poorly gauged mountain basins in Central Spain (Sierra de Gredos), where the lack of instrumental data (flow data) prevents the use of traditional methods for the characterisation of flash floods. In particular, the paper aims to (i) reconstruct the most complete catalogue of past flash floods in the study area, (ii) analyse their frequency, severity, seasonality and synoptic meteorological causes, as well as the human impacts in terms of damage to infrastructures and fatalities, and, in addition, (iii) address the estimation of historical peak discharge, taking into account uncertainties regarding antecedent conditions and land-use changes so that the results of this study can be incorporated into flood risk management.

2. Study region

The basins analysed in this study are located in the eastern Sierra de Gredos massif (Province of Avila) of the Spanish Central System and belong to the basin of the River Tiétar, a tributary of the River Tagus (Fig. 1). Geology in the region is mainly composed of granites (Upper Palaeozoic granitoids) covered by a sandy weathering mantle.

The climate of the study area is Continental Mediterranean, characterised by frequent precipitation in autumn, winter and spring stemming from Atlantic depressions from the SW, and by very dry summers (only 10% of annual precipitation) associated with the presence of the Azores anticyclone. Annual precipitation in the Pelayo basin (800 m asl) is 1913 mm.

Vegetation is abundant in the area and is dominated by *Pinus pinaster* Ait. at the headwaters and deciduous forests (*Quercus pyrenaica* Wahl. and *Quercus ilex* L.) in the lower parts of the study region. European alder (*Alnus glutinosa* L.) and narrow-leaved ash (*Fraxinus angustifolia* Vhal.) predominate in the river corridors. Tree clearance has been practised in the study areas in the past and is still being practised today.

This study focuses on two ungauged basins (those of the River Arenal at Arenas de San Pedro and the River Pelayo) and two poorly gauged basins (the Arenal downstream from Arenas de San Pedro and the River Santa Maria) in the Spanish Central System. The Pelayo

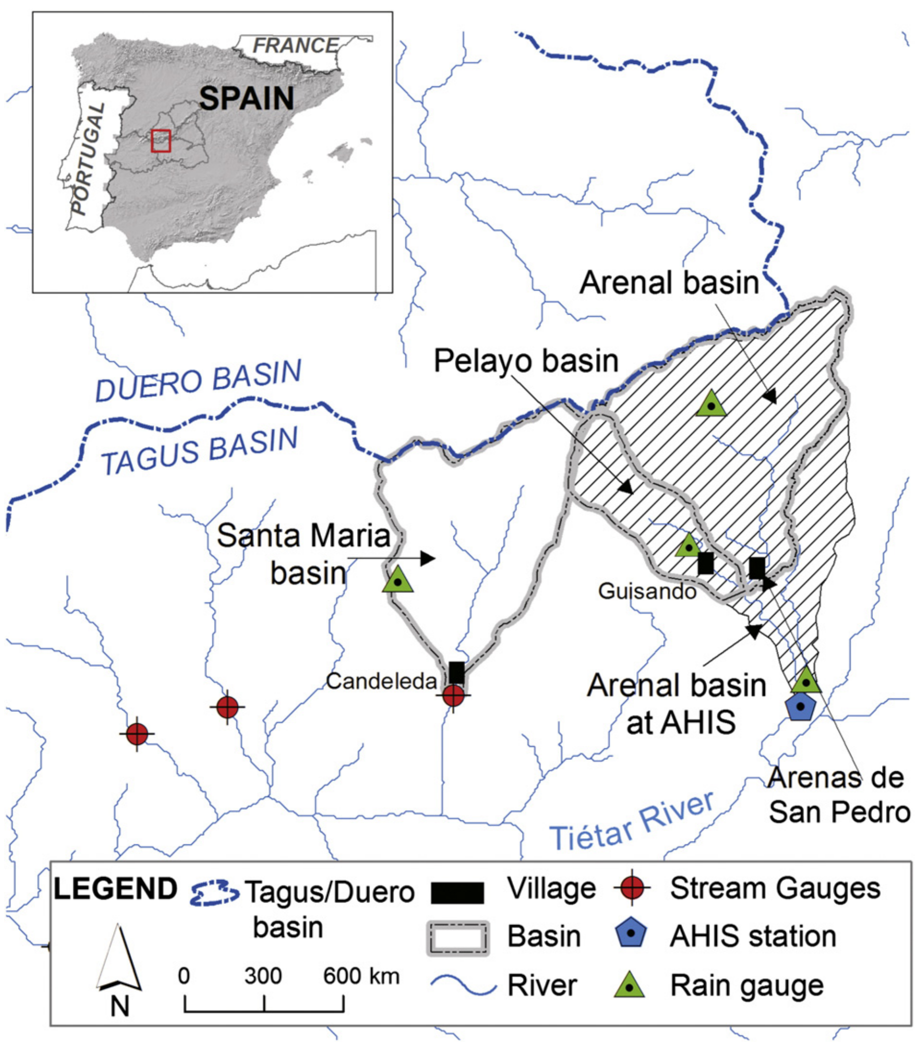

Fig. 1. Location of the four basins analysed: The basins of the Santa María River at Candeleda, the Pelayo at Guisando and the Arenal at Arenas de San Pedro are shown by grey dotted lines and the Arenal River basin at the AHIS station in grey stripes.

Table 1
Main morphometric characteristics of the four basins analysed in this study. Note the existence of an automatic hydrological information system (AHIS) station for the Arenal River and of a stream gauge at Santa Maria River (located in Fig. 1).

	Pelayo River	Arenal River at Arenas de San Pedro	Arenal River at AHIS station	Santa Maria River
Drainage area (km^2)	11.5	67	119	62
River length (km)	5	12.5	21	11
Altitudinal range (m asl)	1460	1800	1941	2017
Average stream slope ($m\ m^{-1}$)	0.29	0.14	0.09	0.18
Time of concentration (h)	1.28	2.95	4.77	2.56

is a tributary of the Arenal; it flows through the village of Guisando (765 inhabitants) and two camp sites. The Arenal is a tributary of the Tiétar and flows through the small town of Arenas de San Pedro (~6900 inhabitants). A stream gauge (automatic hydrological information system [AHIS] station) was installed downstream from the town in 2001 (119 km^2 drainage area). In the neighbouring Santa Maria River basin lies the village of Candeleda (~5145 inhabitants), where a stream gauge has existed since 1973. The main characteristics of these basins are summarised in Table 1.

Although at least 18 people have been killed by floods in the study area and vicinity over the past 70 years, there is still an absence of studies on flood frequency and flood risk management plans for the area.

3. Data acquisition and methods

For the purpose of this study, different approaches were combined and data integrated in order to obtain a detailed characterisation of flash floods in the study area (Fig. 2).

3.1. Historical documentation

Written documentary sources (e.g., municipal archives, newspapers, civil protection documents and scientific papers) were systematically screened to obtain (in-)direct information on the impact that past precipitation and flood events have had on people, goods and services. Qualitative data gathered from these sources were transformed into numerical indices (Barriendos and Coeur, 2004; Bullón, 2011) to derive data on the type, intensity, duration and date of past events.

3.2. Tree-ring analysis

Tree-ring records of 114 *P. pinaster* trees (269 samples) were analysed along a 2.5 km stretch of the River Pelayo upstream of the village of Guisando in order to detect growth disturbances (GD) induced by flash floods. Following the protocol suggested by Ruiz-Villanueva et al. (2010), the dating of flash flood events in the River Pelayo was based on: (i) the nature of GD observed in the tree-ring series (i.e., abrupt growth suppression or release, compression wood, eccentric growth, callus tissue, and injuries), (ii) the intensity of the GD signal in the tree-ring record; (iii) the overall number of trees affected by an event; and (iv) the spatial distribution of affected trees along the stream.

Riparian trees (*A. glutinosa* and *F. angustifolia*) were analysed over a distance of 3 km along the reach of the Arenal River that flows through the town of Arenas de San Pedro. As a result of a clean-up (logging) of the channel by the Water Authority in 2008, 84 cross-sections could be analysed on stumps, thus allowing convenient dating of visible (external) and internal wounds. At the same time, the absence of entire stems prevented an assessment of scar heights and presumably the detection of scars inflicted at higher positions on the stem. As is usual in dendrogeomorphic studies (Stoffel and Bollschweiler, 2008; 2009), additional information was obtained for each tree sampled, namely its geomorphic position, tree coordinates and a description of external disturbances. In the case of the Arenal, the dating of past flood events was accepted if at least two scars were identified in different trees for the same year.

3.3. Instrumental data

The rain gauge network of Central Spain is sparse and unevenly distributed, covering mainly valleys and lowland areas, while mountainous regions have been left behind with very limited data (Buytaert et al., 2006). In addition, the provision of daily data, mainly from hydrometeorological networks in the area, started at best in the

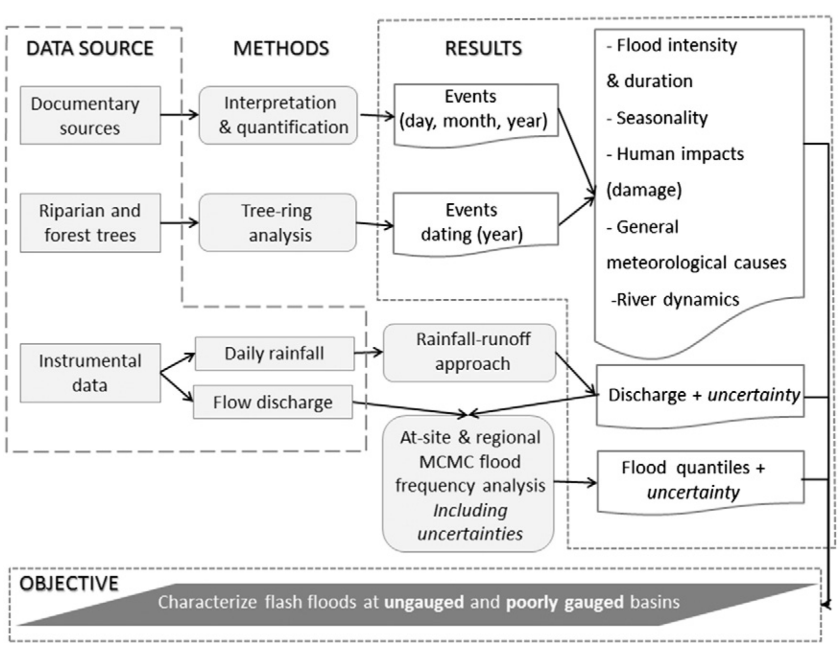

Fig. 2. Methodological flowchart of the study.

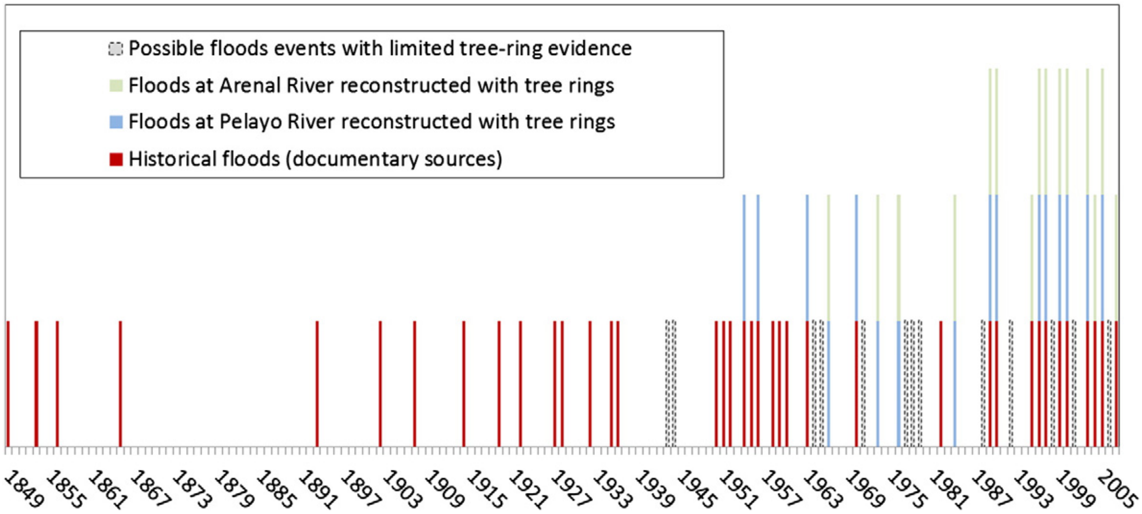

Fig. 3. Regional flood event chronology based on documentary sources and tree ring data from the Pelayo and Arenal rivers.

early twentieth century. Time series usually date only from the 1950s or even later, and the situation in the early 21st century is that many stations have been removed, relocated or have ceased to operate.

This study centres on four rain gauges located in the area (Fig. 1) that provide daily data for the time window covered by documentary and tree-ring sources. In addition, an AHIS station has been operating since 2001, providing subdaily meteorological parameters (flow discharge, rainfall and temperature).

In Spain, the network of flow gauges is very much centred on large river basins, and the few existing records from smaller mountain catchments are usually short and have only existed since 1973 in the studied area.

3.4. Estimation of peak discharge

Unlike the study by Ballesteros Cánovas et al. (2011a, 2011b), where a large number of scars in injured trees could be used to reconstruct peak discharge, flood magnitude in the present case was derived from daily rainfall records.

Daily precipitation data was first transformed into mean areal precipitation for each of the four basins, using inverse distance interpolation (Chow et al., 1988). Precipitation analysis for the period prior to 1950 was approached in a different way. Since only one station was available for the studied area in the early 20th century, the linear regression between this station and the others was tested for the common period and then extrapolated for previous events.

We used the intensity–duration–frequency equation that exists for Spain (Salas and Fernandez, 2007; Temez, 1991) to derive the maximum average intensity for the duration interval equal to the concentration time from daily precipitation. Thus, an empirical rainfall–runoff assessment (rational method) was applied to estimate peak discharge.

To obtain the volume of rainfall leading to surface runoff, the runoff coefficient C is needed ($0 \leq C \leq 1$). The runoff coefficient is a key concept in hydrology and an important diagnostic variable for catchment

Table 2
Discharge estimates (mean and standard deviation) for the four study sites (units are in $m^3\ s^{-1}$).

Date	Arenal R.		Pelayo R.		Arenal R. at AHIS		Arenal R. at AHIS		Santa María R.	
	Mean	STDEV	Mean	STDEV	Mean	STDEV	Q reduced	Error	Mean	STDEV
1936	400	118	109	31	509	145	364	149	509	147
1954	147	40	36	10	153	44	109	45	67	19
1956	69	19	16	5	76	21	55	23	53	15
1958	255	74	58	16	307	93	214	88		
1963	343	102	100	29	435	123	312	128		
1966	213	65	63	19	252	75	177	73	147	43
1969	259	81	88	24	325	97	228	93	116	32
1973	255	77	75	23	313	90	223	91	184	57
1976	232	73	73	23	303	84	219	90	119	34
1982	167	49	50	14	204	57	147	60	106	28
1984	179	56	53	14	216	64	152	62	155	44
1989	230	62	58	17	288	74	214	88		
1995	255	72	62	18	314	90	224	92		
1996	213	60	55	16	261	77	184	75		
1997	340	98	94	27	413	113	300	123		
1999	296	85	83	24	376	108	268	110		
2000	362	97	67	20	333	93	240	98		
2001	166	47	37	11	207	57	150	62		
2002	137	41	50	14	176	50	126	52	74	21
2003	173	51	54	16	211	59	152	62	69	19
2004	153	47	49	13	190	54	136	56	128	37
2005	331	89	101	28	425	114	311	128	389	107
2006	237	69	67	18	313	90	223	91	161	47
2007	139	39	44	14	167	44	123	50	112	33
2008	112	33	29	9	138	40	98	40		
2009	143	40	39	11	186	51	135	55		

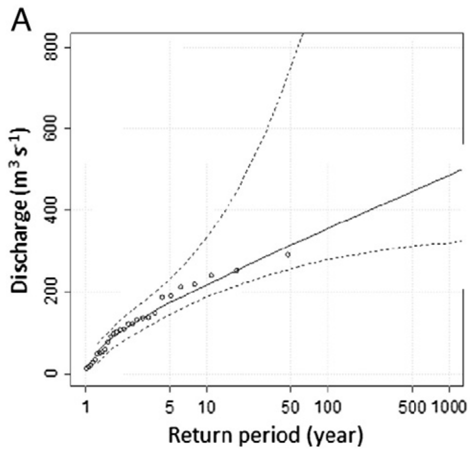

Fig. 4. Fitted GEV distributions: (A) using the instrumental records at the Candeleda station since 1973; (B) using instrumental records and 1936 estimates including uncertainty (length of historical period $h = 70$, perception threshold $X_0 = 300$).

Table 3
Estimation of discharge quantiles' maximum likelihood Q (ML) corresponding to return periods $T = 10$, 50, 100 and 500 years. $CI_{0.05}$ ($CI_{0.95}$) is the 5% (95%) confidence limit of the estimates Q (ML), $\Delta CI = CI_{0.95} - CI_{0.05}$.

T (years)	MCMC settings	Q (ML)	ΔCI	ΔCI / Q_{ML}
10	Only instrumental records	223	166	0.75
	Instrumental + 1936 estimates	211	73	0.35
	1936 as instrumental	264	283	1.07
50	Only instrumental records	330	540	1.63
	Instrumental + 1936 estimates	312	155	0.50
	1936 as instrumental	462	1180	2.55
100	Only instrumental records	377	820	2.18
	Instrumental + 1936 estimates	355	223	0.63
	1936 as instrumental	567	2027	3.57
500	Only instrumental records	487	1962	4.03
	Instrumental + 1936 estimates	456	452	0.99
	1936 as instrumental	876	6596	7.52

response (Marchi et al., 2010). This parameter depends mainly on hydrologic antecedent conditions, land use and soil cover. Since these conditions may not be known in detail for past events, this parameter has been treated as a stochastic variable (using the Monte Carlo method), and the other parameters involved in the rational method (i.e., maximum average intensity, uniformity coefficient and basin area) as deterministic. C was declared a variable with a known uniform distribution over an interval (a, b), where a is the lower bound equal to 0.2, and b is the upper bound equal to 0.6. Selection of these boundaries was based on the values proposed by Marchi et al. (2010), who defined a range of 0.23–0.56 for extreme flash floods in the Mediterranean region.

The 500 Monte Carlo simulations gave results in the form of normalised and cumulative histograms showing the stochastic tendencies of a dataset. A goodness of fit table was then displayed with various probability distributions and the best estimates for their parameters, along with different goodness of fit tests, such as the Kolmogorov–Smirnov test. Final estimated discharges are shown in terms of mean and standard deviation for each simulated event.

The procedure described above was then validated using the records from the stream gauge located in Candeleda and from the Arenal AHIS (for the time period between 2001 and 2008) so as to analyse the accuracy of the approach and the assumed error.

3.5. Incorporation of uncertainties in flood frequency analysis

The flood frequency analysis was applied to three cases with different quantities and types of data: (i) at-site frequency analysis for Candeleda, combining historical information from 1936 and instrumental data series since 1973; (ii) at-site frequency analysis for the Arenal AHIS station, using the short instrumental data series (2001–2011) and longer historical estimates; and (iii) a regional flood frequency analysis (RFFA) using all available flow data from the stream gauges located in the nearby mountains and based on the flood-index method.

For the FFA, a Bayesian Markov Chain Monte Carlo (MCMC) procedure (Reis and Stedinger, 2005) was used, as it can handle information

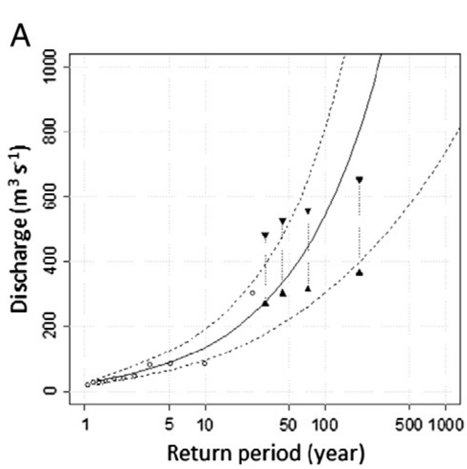

Fig. 5. Fitted GEV distributions based on instrumental data at the River Arenal AHIS station, including (A) the four largest historical events (i.e. the highest magnitude from all estimates) with uncertainty, instrumental records, and (B) all estimates with uncertainty based on historical records.

from historical and instrumental observations in a straightforward way through adequately defined likelihood functions and, more importantly, can account for uncertainties in hydrologic extremes as it provides estimates of confidence bounds for the estimated quantiles (Gaál et al., 2010). We used a code based on the nsRFA package (non-supervised Regional Frequency Analysis) of the R statistical software (Viglione, 2009) specifically developed for FFA. An in-depth description of the method and the fitting procedure can be found in Gaál et al. (2010) and Gaume et al. (2010).

As with the RFFA of Hosking and Wallis (1997), the focus of this analysis was on flood peak and the approach used was the index-flood method of Dalrymple (1960). To carry this out we selected eight stations located in the mountains close to the studied basins. We then applied the assumption of the index-flood method expressed by the equation:

$$Q_i^{(j)} = \mu_i \times q^{(j)}; i = 1, \ldots, M \quad (1)$$

where i denotes a given site, M is the total number of sites in the homogeneous region, $Q_i^{(j)}$ is the jth quantile at the ith site, $q^{(j)}$ is the regional dimensionless (i.e., reduced) jth quantile (i.e., the regional growth curve) and μ_i is the at-site scale factor (i.e., the index flood) that does not depend on j (simple scaling assumption).

To include the estimated discharges from the ungauged studied basins in the RFFA, the index flood has to be related to climatic and/or physiographic watershed characteristics. One of the common models generally used is based on a power law relationship with a single characteristic, which is the catchment area (Gaume et al., 2010). We therefore used this method, although it is possible to use more complex index flood relations.

In the present case, the defined region is not very large and is assumed to be homogeneous in terms of physiography and geography (i.e. main basin characteristics, such as geology, orography and vegetation). Therefore, the hydrological homogeneity of the region was tested only with the Hosking and Wallis method (Hosking and Wallis, 1997).

Once the homogeneous region has been delineated, the discharges, rescaled according to the proposed index flood relation, can be pooled together. The Bayesian MCMC approach was selected to adjust growth curves to these regional sets composed of heterogeneous (instrumental and estimated) data.

The final step was to compare the results of this study with a regional model (called CAUMAX) that is set up for the western part of the Tagus Basin (CEDEX, 2011; Mediero and Jiménez, 2007). This model is proposed for basins of >50 km^2 in this region of the Tagus basin and is based on linear multiple regression:

$$Q_T = 10\alpha_0 \cdot A\alpha_1 \cdot P_m\alpha_2 \cdot H\alpha_3 \quad (2)$$

where A is the basin area, P_m is the maximum precipitation for the estimated return period, H is the mean basin altitude and $\alpha_{1,2,3}$ are the regression coefficients (see the references cited above).

Table 4
Estimation of the discharge quantiles Q (ML) for Arenal River at AHIS station corresponding to the return periods T = 10, 50, 100, 500. $CI_{0.05}$ ($CI_{0.95}$) is the 5% (95%) confidence limit of the estimates Q (ML), $\Delta CI = CI_{0.95} - CI_{0.05}$.

T (years)	MCMC settings	Q (ML)	ΔCI	ΔCI / Q_T
10	Only instrumental records (Inst.)	135	1509	11.17
	Provided by AHIS	262	–	–
	Inst. + threshold > 250[a]	269	159	0.59
	Inst. + threshold > 350[a]	101	81	0.80
	Inst. + 4 major events	154	123	0.79
	Q_red as 'observed'	293	146	0.49
	Q_mean as 'observed'	401	194	0.48
	Historical estimates	244	89	0.36
50	Only instrumental records (Inst.)	396	28,563	72.08
	Provided by AHIS	447	–	–
	Inst. + threshold > 250[a]	519	898	1.73
	Inst. + threshold > 350[a]	229	337	1.46
	Inst. + 4 major events	443	511	1.15
	Q_red as 'observed'	356	363	1.01
	Q_mean as 'observed'	492	487	0.98
	Inst. + historical estimates	408	277	0.68
100	Only instrumental records (Inst.)	629	96,936	154.08
	Provided by AHIS	520	–	–
	Inst. + threshold > 250[a]	664	1794	2.70
	Inst. + threshold > 350[a]	325	639	1.96
	Inst. + 4 major events	692	990	1.43
	Q_red as 'observed'	375	493	1.31
	Q_mean as 'observed'	518	676	1.30
	Inst. + historical estimates	490	456	0.93
500	Only instrumental records (Inst.)	1857	1,799,829	969.17
	Provided by AHIS	–		
	Inst. + threshold > 250[a]	1131	7723	6.82
	Inst. + threshold > 350[a]	731	2825	3.86
	Inst. + 4 major events	1962	4532	2.31
	Q_red as 'observed'	405	896	2.21
	Q_mean as 'observed'	562	1213	2.15
	Inst. + historical estimates	716	1236	1.73

[a] The threshold of 250 (350) m^3 s^{-1} has been exceeding once during the perception threshold.

4. Results

4.1. Flash flood chronology and classification

Results from the Pelayo study showed that the ages of the trees reach up to ~100 years. Scars or injuries were only occasionally found (<10%), whereas other GD was much more frequently observed (280 cases) in the 114 trees investigated. GD was found in 22 of the years, of which eight showed a large number of visible GD in a representative number of trees; information on the flash floods that occurred in these eight years was considered the most accurate of the dataset.

Along the River Arenal, the age of the riparian trees reached up to ~50 years. A total of 147 injuries in 24 different years were detected in the 84 trees analysed. The oldest scar was inflicted in 1953. Several samples contained more than 2 injuries (and up to 7 in the same cross section). The largest number of scars was 16 (11% of the entire population) and corresponded to 1997. Based on the number of trees affected at the same time (and by the same event), reconstruction of past flash floods was considered very reliable for 12 events.

Comparison of tree-ring records from the two catchments shows dendrogeomorphic evidence of flash flood activity in 34 years, which coincided in the two rivers in 14 of these years.

Documentary sources have provided information on 41 events since the 19th century. Of these, the 1936 event should be highlighted here since it was one of the most important floods in the study area. The event was described in archives and newspapers: *The villages of Guisando and Candeleda are completely flooded as a result of the violent storm and flooding. In Guisando village, the flood affected the cemetery and church, removing graves and numerous corpses. In San Esteban del Valle a number of houses were destroyed and several people were left dead or missing.*

The 14 event years identified with tree-ring records from the Pelayo and Arenal rivers were then contrasted with events identified in documentary sources in order to assign each one with an occurrence date. The final database of archival documents used for further analysis therefore contains 41 events (Fig. 3) and is restricted to flash floods registered in documentary sources, events registered in both archival documents and tree-ring series, as well as events simultaneously recorded in a large number of trees but without analogues in written sources.

Fig. 3 also shows periods where information on flash floods is absent from documentary records, because municipality archives are generally missing from 1870 to 1900 and also for the period between 1936 and 1940, presumably as a result of the Spanish Civil War. The apparent increase in flood events since the 1950s, on the other hand, was mainly due to the emergence of various newspapers and the contribution of tree-ring data. An accurate dating of events was possible in 36 cases.

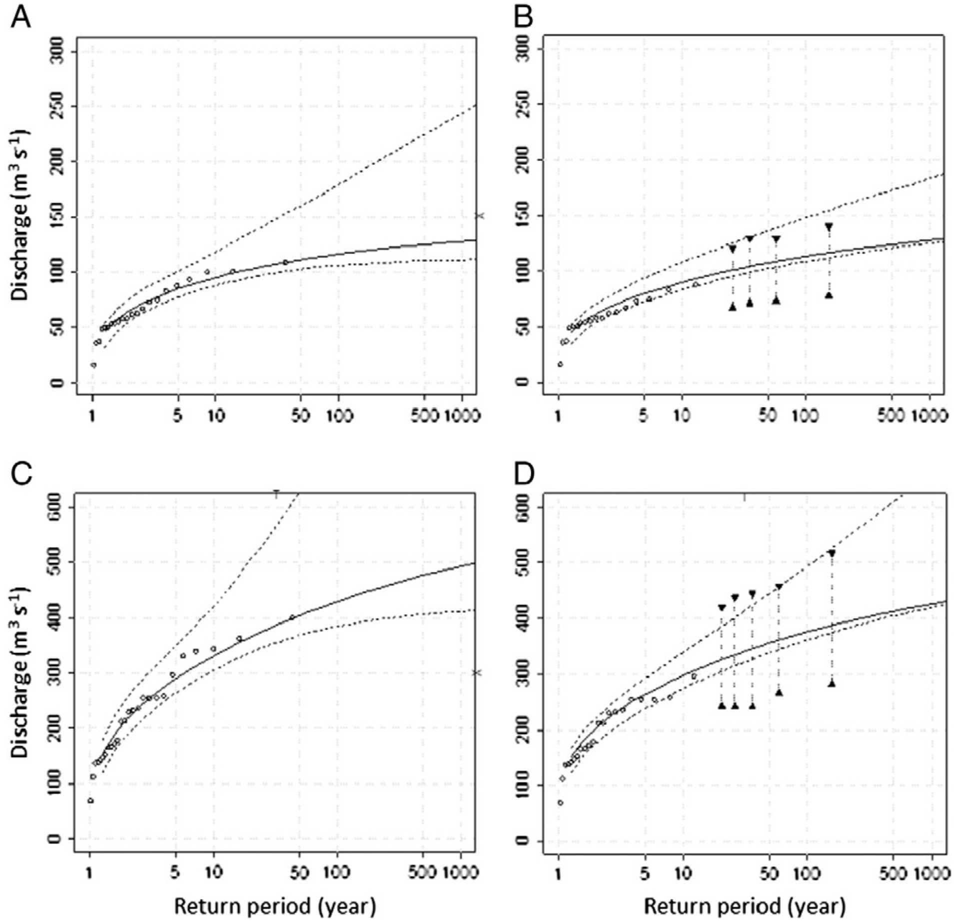

Fig. 6. Fitted GEV distributions for the River Pelayo (A and B) and the River Arenal in the town of Arenas de San Pedro (C and D), with discharge estimates treated as observed records (A and C) and as a combination of part of the data as observed and the 4 (5) largest events with uncertainty (B and D).

4.2. Estimates of flash flood discharges and uncertainties

Results for estimated peak discharges (mean and standard deviations) using the rational method are illustrated in Table 2. The validation of the model for the Candeleda basin and the River Arenal at the AHIS station resulted in a coefficient of determination of 0.83 and 0.85, respectively, a model uncertainty of <17% without significant differences between observation and simulation (p-value < 0.05 at the 95% confidence interval).

For the River Arenal (AHIS station), the lower bound of the calculation (Q reduced in Table 2) was used for the frequency analysis since the dam located on the Cuevas River, as well as a series of dykes and irrigation systems, may influence the discharge.

4.3. Flood frequency analysis

4.3.1. At-site FFA combining historical data and longer instrumental series

The at-site FFA at Candeleda is based on the gauged data on instantaneous discharge (annual maximum) since 1973 and on estimates of the 1936 event along the River Santa Maria at the Candeleda station (Fig. 4).

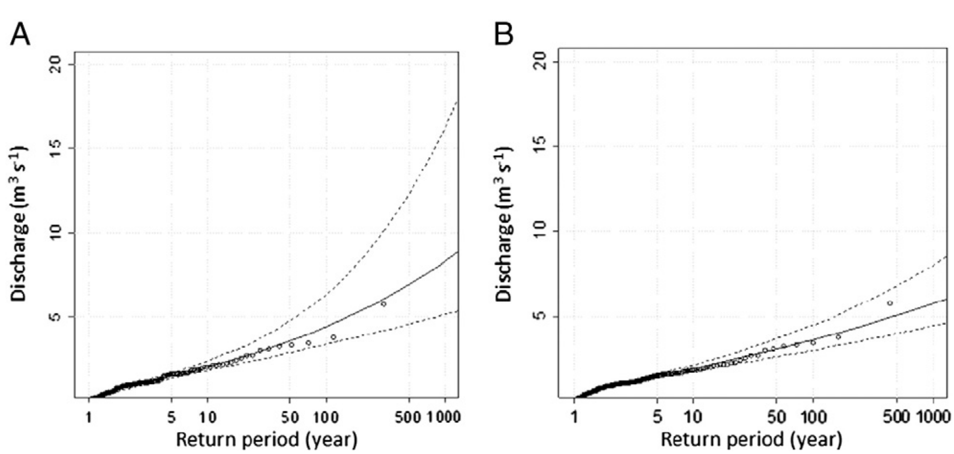

Fig. 7. (A) Regional gauged data set; (B) regional including the whole set of estimated event discharges.

The inclusion of historical information evidently reduces uncertainty in the quantile estimates (Table 3). If the 1936 estimate is treated as instrumental (i.e., without any uncertainty), an increase that is even higher than just the instrumental fitting can be observed in the confidence interval rate, as well as an increase in the quantiles.

4.3.2. At-site FFA using a short data series and longer historical information

The at-site FFA at the River Arenal AHIS station is based on a short data series of annual maximum discharge since 2001 and estimated discharge from longer historical records (Fig. 5), whereby different mechanisms of frequency fitting are applied.

With the inclusion of historical information, uncertainty is evidently reduced in the quantile estimates and homogenised (shown by the line slope), but very significant differences exist in the quantiles depending on the parameters used and the assumptions regarding uncertainty. Table 4 summarises all the tests and compares results with the quantiles provided by the AHIS station.

The main finding from Table 4 is the decrease in the confidence intervals (low values of ΔCI and ΔCI / Q_T in the table) when historical information (estimated discharges and uncertainty range) is included in the analyses together with instrumental records (Inst.).

4.3.3. At-site FFA using only historical information

Instrumental flow records do not exist for the Pelayo and Arenal rivers at Arenas de San Pedro. To use these data for an at-site FFA, several hypotheses were assumed. In a first step, discharge estimates for these reaches were treated as instrumental records ('observed' discharge considering the mean value without uncertainty), and the most important reconstructed floods were then constructed as 'historical' events. The events dataset was thus divided into 'observed' and 'historical' (estimated with uncertainty) in an iterative process. Fig. 6 gives some of the results from this repeating process. These show the variability in quantile estimates based on the way data was incorporated.

The inclusion of some events as historical affects the confidence intervals, and this effect remains visible irrespective of the number of large events included in the analysis (data not shown).

4.3.4. Regional flood frequency analysis (RFFA)

Regional quantiles were estimated based on the index-flood method and the MCMC approach using eight concordant stations from the region. The region defined was assumed to be hydrologically homogeneous (heterogeneity test $H = 1.39$, using the test criteria according to Wallis et al., 2007, which classify regions with $H < 2$ as acceptably homogeneous). A total of 11 probability distribution functions were tested. The generalised extreme value (GEV) function was selected (with the Anderson–Darling goodness of fit test $K = 0.37$) and the estimated initial parameters of GEV function λ_1, λ_2 and λ_3 (location, scale and shape parameters) were 0.6067, 0.5548 and −0.1183 respectively. The MCMC approach was first used for the regional gauged dataset and then used to include the estimates for the three basins (Fig. 7).

5. Discussion

In this study, 41 past floods have been documented based on historical sources and dendrogeomorphic evidence. The veracity of the compiled data is supported by its high level of temporal and spatial coherence and by the correspondence between events described in the documents and those recognised in tree-ring records.

The only available common data between the datasets was daily rainfall, which was consequently used to estimate peak discharge for most of the documented events. We combined an empirical rainfall–runoff assessment with a stochastic approach so as to transform daily data into peak discharge for each event. This simple empirical assessment has been extensively used in Spain (Díez Herrero, 2001; Ortega, 2007; Potenciano, 2004; Rico, 2004) for assessing peak flows in natural watersheds with surface areas up to 3000 km^2 and concentration times ranging from 1 to 24 h. Validation of the method revealed that estimates were associated with 17% error, which is relatively small for past flood reconstructions (peak discharge estimates of historical floods by hydraulic calculations have errors of up to 25%, according to Reis and Stedinger, 2005).

The most important assumption of this study was the treatment of the runoff coefficient as a stochastic variable since antecedent conditions, land use and other parameters are not known for past events. Boundaries (0.2–0.6) were established based on the findings of Marchi et al. (2010), who obtained values in the range of 0.23 to 0.56 for the Mediterranean region. Merz et al. (2007), in contrast, related runoff coefficients with flood type and found that the smallest runoff coefficients (median 0.15) are associated with flash floods and short-rain floods (0.36), whereas slightly larger values are produced by long-term rainfalls (0.38) and the largest runoff coefficients (0.63) are associated with snowmelt floods.

5.1. Interpretation and value of data from documentary sources

Event classification based on documentary sources (archives) proved to be a good approximation to past flood conditions since most of the events classified as high and medium intensity events were indeed related to high flow discharge (1936, 1963, 1995, 1999, 2000, and 2003). The high intensity events were apparently clustered in the early 20th century (i.e., the four most severe events occurred in 1902, 1922, 1927 and 1928). As floods were classified based on damage to infrastructure (bridges and roads) and not on casualties (Barriendos and Coeur, 2004), it seems possible that the great differences in structure quality may have influenced classification. On the other hand, however, events that caused fatalities in the region (i.e., 1936, 1959, 1982, 1990 and 1999) were not necessarily high-intensity (high-magnitude) events but floods that took place in these years during late summer or early autumn, when there is a substantial increase in the population of this region due to tourism.

5.2. Interpretation and value of tree-ring data

Dendrogeomorphic evidence in riparian trees has been used here to date the occurrence and frequency of past floods, but not for a direct estimation of flood magnitude. Although there is no perfect correlation between the number of scarred trees (or growth disturbances) and discharge estimates, we still observe a tendency towards more evidence in trees during larger events, especially along the River Pelayo, where a confidence coefficient (Ruiz-Villanueva et al., 2010) was used rather than the absolute number of injuries (as in the case of the Arenal).

Tree age was the most important limitation of dendrogeomorphology at this study site, as vegetation growing within the area of fluvial activity does not normally reach a high age (<70 years in the present study).

According to Gottesfeld (1996), Zielonka et al. (2008) and Ballesteros Cánovas et al. (2011a, 2011b), scars on trees are most likely to be caused by transported logs and probably by the bedload (boulders and stones). Scar formation generally requires high flow and the presence of debris in the channel. Affected trees may have disappeared from the stream and banks since the last event, either through natural processes or anthropogenic interventions. The series of reconstructed flood events should not therefore be treated as a complete dataset and the total number of growth signatures for each event cannot be used as a direct proxy (St. George, and Nielsen, 2003).

Woody material with different stages of decay and various dimensions was present along the study reach of the River Arenal, as were granite boulders in both the Arenal and Pelayo rivers (boulders are much larger and more abundant in the latter). The large presence of woody debris may explain the predominance of scarred trees along the Arenal and the formation of impacts by floating wood, whereas the scarcity of woody debris and the predominance of bedload transport may explain the rare

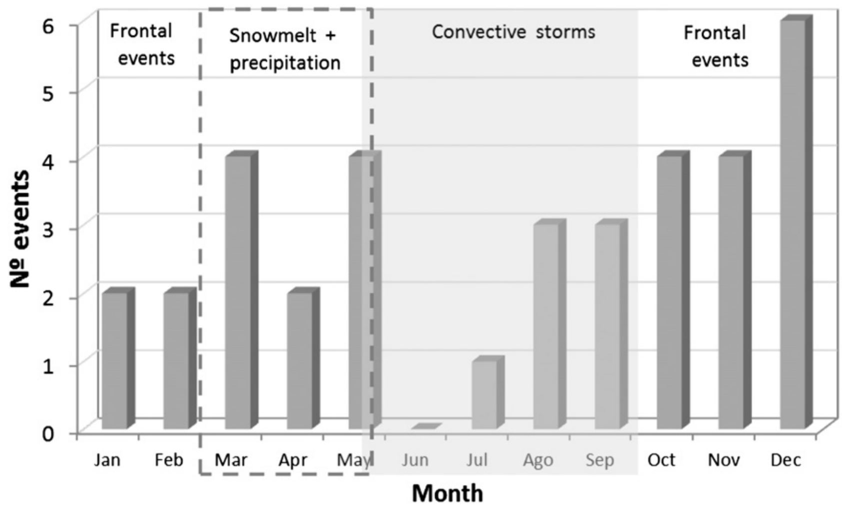

Fig. 8. Seasonality of flash flood events and possible triggering conditions.

occurrence of injuries in trees along the Pelayo. In addition, differences in the composition of tree species (*P. pinaster* trees with thick and protective bark along the Pelayo and more vulnerable thin-barked riparian trees along the Arenal; Stoffel and Perret, 2006; Trappmann and Stoffel, 2013), tree density and river slope may also have contributed to these differences.

Most of the disturbance events recorded in the tree-ring records could be successfully related to documentary information on flood events, and those without analogues in the written archives occurred in the year after the largest events. It is noteworthy that the largest estimated magnitude floods (1936, 1963, 1997, 1999, 2000 and 2005) are in concert with those years best represented in the dendrogeomorphic record for both the Arenal and Pelayo rivers, with the exception of 1936 for which tree age was not sufficient to be recorded in the trees.

For the years in which dendrogeomorphic evidence was clearly visible but documentary information was missing (1966, 1973, 1976, and 1984), we hypothesise that large quantities of recently deposited solids (sediment and wood) could have been remobilised even by moderate flows (*hysteresis* circle). We therefore speculate that dendrogeomorphic evidence is not always necessarily related to extreme events, but that damage can also be inflicted on trees by ordinary high flows. In this regard, provided that tree-ring evidence is used in rivers in the absence of other types of documentary data, dendrogeomorphic time series should be analysed carefully and more in terms of a contribution to river dynamics than as an exclusive indicator of high flows.

5.3. Seasonality, meteorological causes and flood envelopes

The accuracy dating of 36 events made it possible to analyse the seasonality of these floods, which showed that a majority of 60% of events occurred in autumn–winter and 40% in spring–summer (Fig. 8).

The seasonality of floods found in the study region could be related to different meteorological forcings, as shown in Fig. 8, among which three predominate: (i) convective precipitation events occurring in spring and summer, which are locally and temporally limited; (ii) precipitation events caused by wet spells (rain or snowfall) lasting several days or weeks in spring or autumn; and (iii) situations of generally persistent instability lasting for more than a month or an entire season, normally during winter (Benito and Machado, 2012; Bullón, 2011). During this season, zonal circulation at low latitude (35–45°N) generally causes significant and persistent rainfall and floods in the Tagus basin (Benito et al., 2006, 2008; Trigo et al, 2004) in which the study sites are located. At the basin scale, a significant correlation between discharge and the North Atlantic Oscillation (NAO) index can be difficult to identify, but it is still possible to observe a weak trend (based on exploratory analysis and linear regressions) between estimated discharges and the NAO. The most intense events documented here (highest discharges) are correlated with high negative values of the NAO index, such as in 1936 (−3.89), 1966 (−1.69), 1977 (−2.14) and 1996 (−3.78). Flood events in the study region can therefore be associated preferably with wet conditions in the western Mediterranean and over North Africa, and cold air in northern Europe (Wanner et al., 1994).

The seasonality of floods observed in this study also agrees with the distribution documented by Gaume et al. (2009) and Marchi et al. (2010) for European flood events in general and for the Mediterranean region in particular.

For the earlier period (1849–1935), for which discharges could not be estimated, local data was compared with previously published works on the Tagus River basin. According to Benito et al. (2003a, 2003b), the period between 1870 and 1900 shows a substantial increase in the frequency of extraordinary floods in the Tagus basin, whereas Barriendos (1997) identifies a phase between 1840 and 1859 in which a sharp increase in floods and a decrease in droughts were recorded. Similar data also exists for catchments in Eastern and South East Spain (Barriendos and Martín Vide, 1998), particularly for the 1830–1870 period, with a maximum period from 1848 to 1868 and peaks between 1851 and 1857 and in 1859 and 1860, and another period between 1916 and 1951, with peaks between 1917 and 1928. The most exceptional floods affecting the entire Tagus basin were recorded in 1936, 1941 and 1947, as well as in 1917, 1924 and 1928 at its headwaters (Benito et al., 2003a, 2003b). Our findings corroborate the body of evidence on past floods in the Tagus basin and we have also examined the documented events of 1849, 1853, 1856, 1865, 1919, 1922, 1927, 1928 and 1932 in our study region. Their occurrence over large areas leads us to hypothesise that they were at least of medium or high intensity and that they were related to intense rainfall affecting a large part of the Tagus basin.

Our study also shows that the largest magnitude flood of the 20th century in the study area occurred in 1936, when flow records and gauging stations did not exist in the wider study region. We therefore compared the estimates of this flood event with data from the catalogue of maximum observed floods in Spain (IAHS, 2004) and the regional envelope curve (REC). Our analysis shows quite clearly that the 1936 flood was located in the upper bound of the REC (Fig. 9).

If compared with the envelope curves described in the literature for maximum floods in Europe (Castellarin, 2007; Gaume et al.,

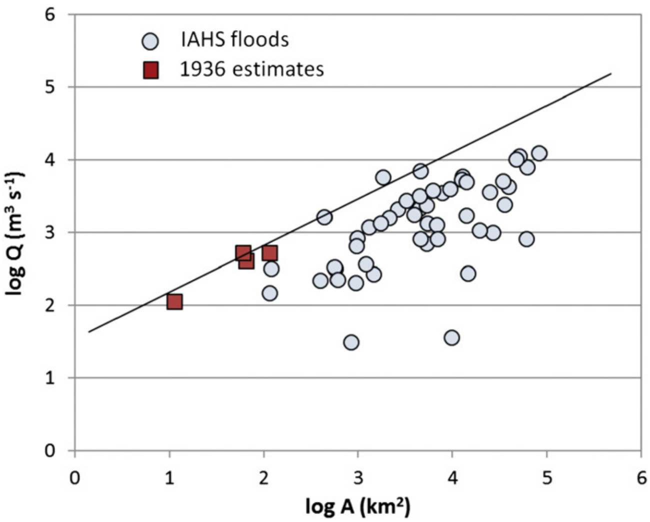

Fig. 9. Catalogue of maximum observed floods in Spain (IAHS, 2004) and estimates of the 1936 flood in the study region (four catchments analysed). The black line represents the regional envelope curve (REC) of the IAHS database.

2009; Marchi et al., 2010; Tarolli et al., 2012), discharge per unit area of the 1936 event will fall below these curves, with an approximate envelope curve equation: $Q_u = 20.82 \cdot A^{-0.29}$.

5.4. Flash flood frequency

As a final analytical step, this study aimed to incorporate data on historical floods gathered from documentary sources and tree-ring records into an at-site and regional flood frequency analysis (FFA and RFFA, respectively). For this purpose, a Bayesian Markov Chain Monte Carlo (MCMC) framework was used (Gaál et al., 2010; Gaume et al., 2010; Kuczera, 1999; Reis and Stedinger, 2005) and a likelihood function was built so as to properly handle the information on historical floods. Following Gaume et al. (2010), we considered that accurate data on extremes (in terms of discharge) are not absolutely necessary in such analyses as the dominant information needed is the number of non-exceedances of a perception threshold (X_0) and the historical period (h). We set these two parameters following the methodology proposed by Gaál et al. (2010).

The flood of 1936 presented a challenge to our study as this event was larger than any discharge recorded during the periods covered by continuous hydrological records and therefore influenced flood frequency analyses. In the Santa Maria basin at Candeleda village, for instance, the inclusion of historical information evidently reduces uncertainty and affects quantile estimates. The relatively small reduction in quantiles may be explained by the fact that the historical estimate of the 1936 event is affected by relatively large errors (Reis and Stedinger, 2005), but results that include this historical extreme still seem more reliable since confidence bounds are significantly reduced.

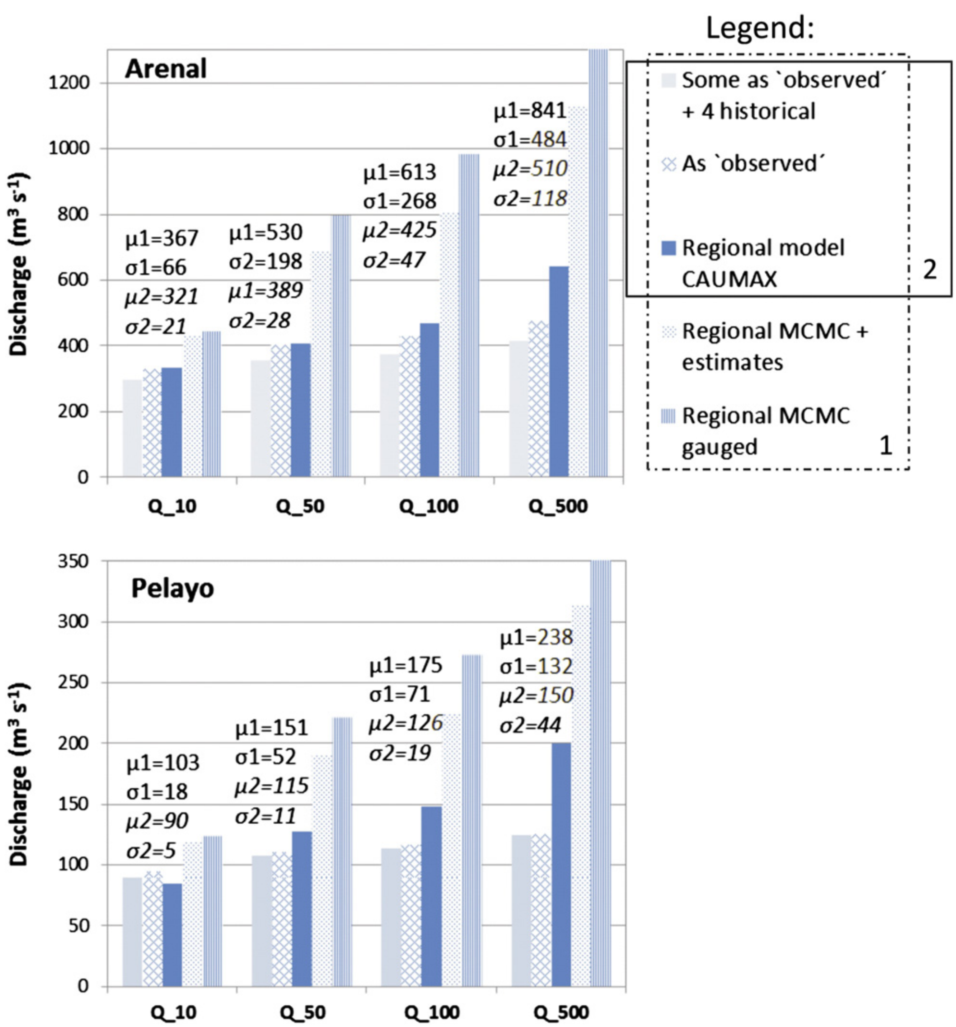

Fig. 10. Discharge for different return periods for all FFA and RFFA tests in the ungauged basins. $\mu1$ and $\sigma1$ are the mean and standard deviations for each return period computing all tests, and $\mu2$ and $\sigma2$ are the mean and standard deviations for at-site tests and CAUMAX but without RFFA (see legend).

The particular case of the River Arenal at the AHIS station is the most difficult to address with the available data. A short data series exists, and a longer series of historical estimates has been incorporated in different ways. In all cases, quantiles provided by the regional approach seem to be slightly underestimated when compared with the CAUMAX model, but they generally remain within the same order of magnitude and within the confidence intervals.

The most important differences between conventional series and those that include tree-ring and documentary sources are found in the regional approach, for which larger quantiles are observed. This is similar to the findings of Gaume et al. (2010) for the Gard region in France, where the quantile estimation, including ungauged events, was multiplied by a factor of >2, presumably because of a limited set of ungauged events and the short period covered by the gauged series. Fig. 10 illustrates differences in quantile estimation based on different approaches, and the related uncertainties expressed by μ and σ (mean and standard deviation of quantiles).

Note how estimation of the largest quantiles (500 years) may be strongly affected (up to twice the value) depending on the treatment of the data (Fig. 10). Underestimation may result in an underestimation of risk, but at the same time overestimation could also result in an economic overestimation in risk management. Because of this uncertainty in the quantile estimation, flood hazard maps may be conceived using a probability approach (Bates et al., 2004; Pappenberger et al., 2006; Romanowicz and Beven, 2003), as deterministic approaches normally do not take uncertainties into account (Bates et al., 2004; Di Baldassarre et al., 2010; Merz and Bloschl, 2005; Merz et al., 2007).

6. Conclusions

This study focused on the reconstruction of ‘real floods’ occurring in small ungauged or poorly gauged mountain basins of Central Spain. Historical documents allowed the analysis of flood seasonality and inferred meteorological causes. In addition, tree-ring records were used to complement documentary sources as well as to improve the understanding of river dynamics.

An empirical rainfall–runoff method was combined with a stochastic approach in order to incorporate uncertainty related to past land uses or antecedent conditions during past events. Through the incorporation of (several subsets of) data on historical floods with associated uncertainty, we calculated different FFA and RFFA and evaluated the influence of varying approaches on the estimation of quantiles in at-site and regional analyses. The study successfully demonstrated that uncertainty decreases if historical data is included, but that quantile estimates can be affected quite strongly depending on the approach used. This uncertainty should be taken into account when historical data is used for flood risk purposes or management plans. Although this study is focused on only four basins, we are confident that the proposed methods can be easily transposed to any other ungauged or poorly gauged basin.

Acknowledgements

The authors would like to express their gratitude to the Spanish Ministry of Science and Innovation for its financial support. The work was funded by the MAS Dendro-Avenidas project (CGL2010-19274) and the Geological Survey of Spain (IGME). We are grateful to the Tagus Water Authority and the Meteorological Agency (AEMET) for meteorological data, and to the Environment Department of Castilla y León in Ávila, and the Arenas de San Pedro and Guisando Councils (particularly to Nuria Blázquez, Gloria Suárez and Sixto Díaz) for their collaboration. Our special thanks go to Fernando Palacios for providing historical data and to TRAGSA for sampling the cross-sections of trees. The authors also wish to express their gratitude to J.A. Fernández-Yuste for his helpful comments on frequency analysis and Prof. Marco Borga and other anonymous reviewers for their insightful comments.

References

Alestalo, J., 1971. Dendrochronological Interpretation of Geomorphic Processes. Fennia.
Arbellay, E., Fonti, P., Stoffel, M., 2012. Duration and extension of anatomical changes in wood structure after cambial injury. Journal of Experimental Botany 63, 3271–3277.
Ballesteros Cánovas, J.A., Bodoque, J.M., Díez-Herrero, A., Sanchez-Silva, M., Stoffel, M., 2011a. Calibration of floodplain roughness and estimation of palaeoflood discharge based on tree-ring evidence and hydraulic modelling. Journal of Hydrology 403, 103–115.
Ballesteros Cánovas, J.A., Eguibar, M., Bodoque, J.M., Díez-Herrero, A., Stoffel, M., Gutiérrez-Pérez, I., 2011b. Estimating flash flood discharge in an ungauged mountain catchment with 2D hydraulic models and dendrogeomorphic paleostage indicators. Hydrological Processes 25, 970–979.
Ballesteros, J.A., Stoffel, M., Bodoque, J.M., Bollschweiler, M., Hitz, O., Díez-Herrero, A., 2010a. Wood anatomy of *Pinus pinaster* Ait. following wounding by flash floods. Tree-Ring Research 66, 93–103.
Ballesteros, J.A., Stoffel, M., Bollschweiler, M., Bodoque, J.M., Díez-Herrero, A., 2010b. Flash-flood impacts cause changes in wood anatomy of *Alnus glutinosa*, *Fraxinus angustifolia* and *Quercus pyrenaica*. Tree Physiology 30, 773–781.
Barriendos, M., 1997. Climatic variations in the Iberian Peninsula during the late Maunder Minimum (AD 1675–1715): an analysis of data from rogation ceremonies. The Holocene 7 (1), 105–111.
Barriendos, M., Coeur, D., 2004. Flood data reconstruction in historical times from non-instrumental sources in Spain and France. In: Benito, G., Thorndycraft, V.R. (Eds.), Systematic, Palaeoflood and Historical Data for the Improvement of Flood Risk Estimation. Methodological Guidelines. Centro de Ciencias Medioambientales, Madrid, Spain, pp. 29–42.
Barriendos, M., Martín Vide, J., 1998. Secular climatic oscillations as indicated by catastrophic floods in the Spanish Mediterranean coastal area (14th–19th centuries). Climatic Change 38, 473–491.
Bates, P.D., Horritt, M.S., Aronica, G., Beven, K., 2004. Bayesian updating of flood inundation likelihoods conditioned on flood extent data. Hydrological Processes 18, 3347–3370.
Benito, Machado, 2012. Floods in the Iberian Peninsula. Changes in Flood Risk in Europe IAHS Special Publ. 10.
Benito, G., Thorndycraft, V.R., 2005. Palaeoflood hydrology and its role in applied hydrological sciences. Journal of Hydrology 313, 3–15.
Benito, G., Díez, A., Fernández de Villalta, M., 2003a. Magnitude and frequency of flooding in the Tagus basin (Central Spain) over the last millennium. Climatic Change 58, 171–192.
Benito, G., Sanchez-Moya, Y., Sopeña, A., Machado, M.J., Pérez Gonzalez, A., 2003b. Palaeoflood record of the Tagus River (Central Spain) during the late Pleistocene and Holocene. Quaternary Science Reviews 22, 1737–1756.
Benito, G., Thorndycraft, V.R., Enzel, Y., Sheffer, N.A., Rico, M., Sopeña, A., Moya, Y., 2004. Palaeoflood data collection and analysis. In: Benito, G., Thorndycraft, V.R. (Eds.), Systematic, Palaeoflood and Historical Data for the Improvement of Flood Risk estimation. Methodological Guidelines. CSIC, Madrid, pp. 15–28.
Benito, G., Rico, M., Thorndycraft, V.R., Sánchez-Moya, Y., Sopeña, A., DíezHerrero, A., Jiménez, A., 2006. Palaeoflood records applied to assess dam safety in SE Spain. RiverFlow. Balkema (Taylor & Francis Group), Oxford, UK.
Benito, G., Thorndycraft, V.R., Rico, M., Sánchez-Moya, Y., Sopeña, A., 2008. Palaeoflood and floodplain records from Spain: evidence for long-term climate variability and environmental changes. Geomorphology 101, 68–77.
Brázdil, R., Pfister, C., Wanner, H., Storch, H., Luterbacher, J., 2005. Historical climatology in Europe — the state of the art. Climatic Change 70, 363–430.
Brázdil, R., Kundzewicz, Z.W., Benito, G., 2006. Historical hydrology for studying flood risk in Europe. Hydrological Sciences Journal 51, 739–764.
Brázdil, R., Pfister, C., Wanner, H., von Storch, H., Luterbacher, J., 2010. Historical climatology in Europe — the state of the art. Climate Change 70, 7–40.
Bullón, 2011. Relationships between precipitation and floods in the fluvial basins of Central Spain based on documentary sources from the end of the16th century. Natural Hazards and Earth System Science 11, 2215–2225.
Buytaert, W., Celleri, R., Willems, P., Bièvre, B.D., Wyseure, G., 2006. Spatial and temporal rainfall variability in mountainous areas: a case study from the south Ecuadorian Andes. Journal of Hydrology 329, 413–421.
Castellarin, A., 2007. Probabilistic envelope curves for design flood estimation at ungauged sites. Water Resources Research. 43, 4.
CEDEX, 2011. Mapa de caudales máximos. Memoria técnica.
Chow, V.T., Maidment, D., Mays, L.W., 1988. Applied Hydrology. McGraw-Hill, New York.
Dalrymple, T., 1960. Flood frequency analysis. US Geological Survey Water Supply Paper, p. 1543A.
Di Baldassarre, G., Schumann, G., Bates, P.D., Freer, J., Beven, K., 2010. Floodplain mapping: a critical discussion on deterministic and probabilistic approaches. Hydrological Sciences Journal 55, 364–376.
Díez Herrero, A., 2001. Geomorfología e Hidrología fluvial del río Alberche. Modelos y SIG para la gestión de riberas. Tesis doctoral. Universidad Complutense de Madrid (unpublished).
Díez-Herrero, A., Ballesteros-Cánovas, J.A., Bodoque, J.M., Ruiz-Villanueva, V., in press. A new methodological protocol for the use of dendrogeomorphological data in flood risk analysis. Hydrology Research.

Gaál, L., Szolgay, J., Kohnová, S., Hlavcová, K., Viglione, A., 2010. Inclusion of historical information in flood frequency analysis using a Bayesian MCMC technique: a case study for the power dam Orlík, Czech Republic. Contributions to Geophysics and Geodesy 40, 121–147.

Gaume, E., Valerie, B., Pietro, B., Newinger, O., Barbuc, M., Bateman, A., Blâskovicová, L., Blöschl, G., Borga, M., Dumitrescu, A., Daliakopoulos, J., Garcia, J., Irimescu, A., Kohnova, S., Koutroulis, A., Marchi, L., Matreata, S., Medina, V., Preciso, E., Sempere-Torres, D., Stancalie, G., Szolgay, J., Tsanis, I., Velasco, D., Viglione, A., 2009. A compilation of data on European flash floods. Journal of Hydrology 367, 70–78.

Gaume, E., Gaál, L., Viglione, A., Szolgay, J., Kohnov'a, S., Blöschl, G., 2010. Bayesian MCMC approach to regional flood frequency analyses involving extraordinary flood events at ungauged sites. Journal of Hydrology 394, 101–117.

Gottesfeld, S., 1996. British Columbia flood scars: maximum flood-stage indicators. Geomorphology 14, 319–325.

Hosking, J.R.M., Wallis, J.R., 1997. Regional Frequency Analysis. Cambridge University Press (224 pp.).

International Association of Hydrological Sciences (IAHS), 2004. World Catalogue of Maximum Observed Floods. IAHS Press.

Johnson, R.M., Warburton, J., 2002. Flooding and geomorphic impacts in a mountain torrent: Raise Beck, central Lake District, England. Earth Surface Processes and Landforms 27, 945–969.

Kuczera, 1999. Comprehensive at-site flood frequency analysis using Monte Carlo Bayesian inference. Water Resources Research 35 (5), 1551–1557.

Marchi, L., Borga, M., Preciso, E., Gaume, E., 2010. Characterisation of selected extreme flash floods in Europe and implications for flood risk management. Journal of Hydrology 394, 118–133.

Martín-Vide, J., Barriendos, M., 1995. The use of rogation ceremony records in climatic reconstruction. A case study from Catalonia Spain. Climatic Change 30, 201–221.

Mediero, L., Jiménez, A., 2007. Regional analysis for frequency estimation of annual flood peaks in ungauged basins of Spain. EGU2007-A-03251. Abstracts of the Contributions of the EGU General Assembly 2007, Vienna (Austria), 15–20 April 2007. European Geosciences Union1029-7006.

Merz, R., Bloschl, G., 2005. Flood frequency regionalization spatial proximity vs. catchment attributes. Journal of Hydrology 302, 283–306.

Merz, B., Thieken, A.H., Gocht, M., 2007. Flood risk mapping at the local scale: concepts and challenges. In: Begum, S., Stive, M.J.F., Hall, J.W. (Eds.), Flood Risk Management in Europe: Innovation in Policy and Practice. Series: Advances in Natural and Technological Hazards Research, 25. Springer, Dordrecht, pp. 231–251 (Chapter 13).

Ortega, J.A., 2007. Paleocrecidas, avenidas recientes e hidroclimatología en la cuenca media y baja del rio Guadiana. Tesis doctoral. Universidad Complutense de Madrid (unpublished).

Pappenberger, F., Matgen, P., Beven, K.J., Henry, J.B., Pfister, L., de Fraipont, P., 2006. Influence of uncertain boundary conditions and model structure on flood inundation predictions. Advances in Water Resources 29, 1430–1449.

Potenciano, A., 2004. Las inundaciones históricas en el centro-sur de la Península Ibérica. Condicionantes geomorfológicos y climáticos. Tesis doctoral. Universidad Complutense de Madrid (unpublished).

Reis, D.S., Stedinger, J.R., 2005. Bayesian MCMC flood frequency analysis with historical information. Journal of Hydrology 313 (1–2), 97–116.

Rico, M., 2004. Las paleocrecidas en la cuenca media del Río Segre durante el Pleistoceno superior-Holoceno: registros morfosedimentarios y análisis hidroló-gico. Tesis doctoral. Universidad de Zaragoza (unpublished).

Rico, M., Benito, G., Barnolas, A., 2001. Combined palaeoflood and rainfall–runoff assessment of mountain floods (Spanish Pyrenees). Journal of Hydrology 245 (1–4), 59–72.

Romanowicz, R., Beven, K., 2003. Estimation of flood inundation probabilities as conditioned on event inundation maps. Water Resources Research 39 (3), 1073–1085.

Ruiz-Villanueva, V., Díez-Herrero, A., Stoffel, M., Bollschweiler, M., Bodoque, J.M., Ballesteros, J.A., 2010. Dendrogeomorphic analysis of flash floods in a small ungauged mountain catchment (Central Spain). Geomorphology 118, 383–392.

Salas, L., Fernandez, T., 2007. In-site regionalization to estimate an intensity - duration - frequency law: a solution to scarce spatial data in Spain. Hydrological Processes 21, 3507–3513.

St. George,, S., Nielsen, E., 2003. Palaeoflood records for the Red River, Manitoba, Canada, derived from anatomical tree-ring signatures. Holocene 13 (4), 547–555.

Stoffel, M., Bollschweiler, M., 2008. Tree-ring analysis in natural hazards research — an overview. Natural Hazards and Earth System Sciences 8, 187–202.

Stoffel, M., Bollschweiler, M., 2009. What tree rings can tell about earth-surface processes. Teaching the principles of dendrogeomorphology. Geography Compass 3, 1013–1037.

Stoffel, M., Perret, S., 2006. Reconstructing past rockfall activity with tree rings: some methodological considerations. Dendrochronologia 24, 1–15.

Stoffel, M., Wilford, D.J., 2012. Hydrogeomorphic processes and vegetation: Disturbance, process histories, dependencies and interactions: Earth Surface Processes and Landforms, v.37, pp. 9–22. http://dx.doi.org/10.1002/esp.2163.

Tarolli, P., Borga, M., Morin, E., Delrieu, G., 2012. Analysis of flash flood regimes in the North-Western and South-Eastern Mediterranean regions. Natural Hazards and Earth System Science 12 (5), 1255–1265.

Temez, J.R., 1991. Extended and improved rational method. Version of the Highways Administration of Spain. Proc.XXIV Congress. España, vol. A (33–40 pp.).

Thorndycraft, V.R., Barriendos, M., Benito, G., Rico, M., Casas, A., 2006. The catastrophic floods of AD 1617 in Catalonia (northeast Spain) and their climatic control. Hydrological Sciences Journal 51 (5), 899–912.

Trappmann, D., Stoffel, M., 2013. Counting scars on tree stems to assess rockfall hazards: a low effort approach, but how reliable? Geomorphology 180–181, 180–186.

Trigo, R.M., Pozo-Vazquez, D., Osborn, T.J., Castro-Díez, Y., Gámis-Fortis, S., Esteban-Parra, M.J., 2004. North Atlantic Oscillation influence on precipitation, river flow and water resources in the Iberian Peninsula. International Journal of Climatology 24, 925–944.

Viglione, A., 2009. nsRFA: non-supervised regional frequency analysis. R Package.

Wallis, J.R., Schaefer, M.G., Barker, B.L., Taylor, G.H., 2007. Regional precipitation frequency analysis and spatial mapping for 24-hour and 2-hour durations for Washington State. Hydrology and Earth System Sciences 11 (1), 415–442.

Wanner, H., Brazdil, R., Frich, P., Frydendahl, K., Jonsson, T., Kington, J.A., Pfister, C., Rosenorn, Wishman, E., 1994. Synoptic interpretation of monthly weather maps for the late Maunder Minimum. In: Frenzel, B., Pfister, C., Glaser, B. (Eds.), Climatic Trends and Anomalies in Europe, pp. 1675–1704.

Yanosky, T.M., Jarrett, R.D., 2002. Dendrochronologic evidence for the frequency and magnitude of paleofloods. Ancient floods, modern hazards: principles and application of paleoflood hydrology. Water Science and Application 5, 77–89.

Zielonka, T., Holeksa, J., Ciapala, S., 2008. A reconstruction of flood events using scarred trees in the Tatra Mountains, Poland. Dendrochronologia 26, 173–183.